Modélisation numérique régionale de l'impact des éoliennes offshore sur l'hydrodynamique et le transport sédimentaire

Aurélie Rivier, Anne-Claire Bennis, Grégory Pinon, Markus Gross, Vanessa Magar

14èmes Journées de l'Hydrodynamique

18-19-20 novembre 2014

DGA Techniques hydrodynamiques
Chaussée du Vexin
27105 Val de Reuil

MODELISATION NUMERIQUE REGIONALE DE L'IMPACT DES EOLIENNES OFFSHORE SUR L'HYDRODYNAMIQUE ET LE TRANSPORT SEDIMENTAIRE

REGIONAL NUMERICAL MODELLING OF OFFSHORE WIND TURBINE IMPACTS ON HYDRODYNAMICS AND SEDIMENT TRANSPORT

A. RIVIER[1], A. C. BENNIS[1], G. PINON[2], M. GROSS[3], V. MAGAR[3]

1 Laboratoire de Morphodynamique continentale et côtière, UMR CNRS 6143 M2C, Université de Caen Basse-Normandie, Caen, France
aurelie.rivier@unicaen.fr

2 Laboratoire Ondes et Milieux Complexes, UMR CNRS 6294 LOMC, Université du Havre, 53, Rue Prony, CS 80 540, 76058 Le Havre, France.

3 Departamento de Oceanografía Física, CICESE
Carretera Ensenada-Tijuana No. 3918, CP 22860, Ensenada, B.C., México.

Résumé

L'objectif de ce travail est de représenter correctement dans un modèle numérique l'impact des fondations d'éoliennes offshore de type monopile sur la circulation et le transport sédimentaire à l'échelle régionale. Le modèle de circulation régionale MARS3D est appliqué sur la zone du futur site éolien de Courseulles-sur-Mer (Calvados, France). Les éoliennes sont prises en compte dans le modèle en utilisant deux approches. La première méthode consiste à tenir compte directement des éoliennes dans le maillage et la seconde à paramétrer cet impact en ajoutant des termes sources dans les équations du moment et dans les équations du modèle de turbulence k-epsilon. Les résultats issus des deux techniques sont comparées. Les deux méthodes montrent l'impact attendu sur la circulation. Une zone de décélération est observée en amont et en aval de la pile alors que les courants sont accélérés sur les côtés. Le lit sédimentaire est érodé dans les zones où le courant est accéléré par la présence de la monopile, entraînant une augmentation de la concentration de sédiment en suspension.

Summary

The purpose of this work is to find a parameterization which is able to represent properly the modifications caused by offshore wind turbines foundations on the hydrodynamics and sediment transport at regional scales. As a case study, the regional hydro-sedimentary model MARS3D is applied on an area including the future offshore wind farm of Courseulles-sur-Mer (Normandy, France). Turbines are represented in the model

using two approaches. The first method takes into account monopiles directly in the mesh as dry cells and the second one uses a sub-grid parameterization method by adding drag force term in momentum equations and source terms in k-ϵ turbulence model equations. Comparisons between the results obtained by the different approaches are carried out. As expected, both show impacts on the circulation, with formation of a wake downstream, flow deceleration in front of the pile, and flow acceleration at the side edges. Near-bed erosion occurs in locations where current speeds increase due to the monopile presence, leading to an increase of suspended sediment concentration.

I – Introduction

The construction of several offshore wind farms in the English Channel is planned in the coming years. They will be located both along French and English coasts (projects offshore of Saint-Brieuc, Fécamp, Courseulles-sur-Mer, Isle of Wight and Hasting). Although no wind turbines are present in the English Channel at the moment, they are numerous in the North Sea, where their impacts on sediment transport have been observed in a number of studies (e.g. [8, 10, 22]). The effects of offshore monopiles on local hydrodynamics have been evaluated in environmental impact studies using analytical expressions of drag (e.g. [11]), or with finite element models in two dimensions (e.g. [3]). The first approach is simplistic, and the second one doesn't solve the vertical structure of velocity and therefore the near-bed velocity, which plays a key role for sediment transport. The aim of this work is to estimate monopile impact on the hydrodynamics and sediment transport in three dimensions in regional models like MARS [12]. In these models, the typical spatial resolution allowing for reasonable calculation time is too coarse for explicitly incorporating the monopiles at a regional scale. The first step, described in this paper, consists in evaluating the impacts using the regional circulation model MARS 3D with a higher spatial resolution in a small area. The first strategy explicitly solves the wind turbine and the second one is based on a subgrid parameterization of the wind turbine effects on the environment. The study focuses on the area of the future wind farm of Courseulles-sur-Mer, where the bed is composed of sand and gravels and the water depth is between 20 and 30 meters (m). Currents induced by tide are strong, reaching speeds of 1 meter per second (m/s) during medium spring tides. The influence of waves is weaker in the wind farm site, because the area is protected against waves from the Atlantic Ocean by the Cotentin Peninsula. This paper presents preliminary results obtained with both strategies in a test case having characteristics close to Courseulles-sur-Mer site. Then these methods are applied in the real case using nested ranks.

II – Model description

The regional hydrodynamical model MARS3D [12] and its sediment transport module [13] are applied in this study. It solves the momentum equations under the Boussinesq and the hydrostatic approximation which is expressed in a Cartesian coordinates system as :

$$\frac{\partial u}{\partial t} + u\frac{\partial u}{\partial x} + v\frac{\partial u}{\partial y} + w\frac{\partial u}{\partial z} - fv = -\frac{1}{\rho_0}\frac{\partial p}{\partial x} + \frac{1}{\rho_0}\left(\frac{\partial \tau_{xx}}{\partial x} + \frac{\partial \tau_{xy}}{\partial y} + \frac{\partial \tau_{xz}}{\partial z}\right) \quad (1)$$

$$\frac{\partial v}{\partial t} + u\frac{\partial v}{\partial x} + v\frac{\partial v}{\partial y} + w\frac{\partial v}{\partial z} + fu = -\frac{1}{\rho_0}\frac{\partial p}{\partial y} + \frac{1}{\rho_0}\left(\frac{\partial \tau_{yx}}{\partial x} + \frac{\partial \tau_{yy}}{\partial y} + \frac{\partial \tau_{yz}}{\partial z}\right) \quad (2)$$

with $\mathbf{u}(u, v, w)$ the velocity vector, f the Coriolis parameter, ρ_0 the reference density, p the pressure, and τ the Reynolds stress tensor.

Vertical mixing is solved using the generic length scale formulation [21]. The turbulence equations are the following :

$$\frac{\partial k}{\partial t} + u\frac{\partial k}{\partial x} + v\frac{\partial k}{\partial y} = \frac{\partial}{\partial z}\left(\frac{\nu_V}{s_k}\frac{\partial k}{\partial z}\right) + P + B - \epsilon \tag{3}$$

$$\frac{\partial \psi}{\partial t} + u\frac{\partial \psi}{\partial x} + v\frac{\partial \psi}{\partial y} = \frac{\partial}{\partial z}\left(\frac{\nu_V}{s_\psi}\frac{\partial \psi}{\partial z}\right) + \frac{\psi}{k}(C_1 P + C_3 B - C_2 \epsilon F_{wall}) \tag{4}$$

where k is the turbulent kinetic energy, ψ is a generic length scale, P and B represent the effects of shear and buoyant production, C_1, C_2, C_3, s_k, s_ψ are empirical constants. Buoyancy is neglected in this study ($B = 0$). For a $k - \epsilon$ turbulence model, they are adopted as follows $C_1 = 1.44$, $C_2 = 1.92$, $s_k = 1$, $s_\psi = 1.3$ and F_{wall} is equal to 1 [21]. Horizontal viscosity depends on the size of the mesh and it is expressed as :

$$\nu_H = f_{visc} \cdot 0.01 \cdot \Delta y^{1.15} \tag{5}$$

with f_{visc} a coefficient ranging between 1 and 17 and Δy being the size of the cell in y-direction.

As explained before, the influence of the monopile is taken into account using two methods. In the first one, the monopiles are solved explicitly. They are incorporated in the mesh and are treated as dry cells in the model. In the second one, the impact of the foundations on the environment is parameterized. The drag force exerted on the flow by the monopile is incorporated in the model by adding an extra source term in the momentum and turbulence equations. This second approach was already used to model the impact of vegetation on flow [20, 7, 5]. The drag force per unit area, $\mathbf{F_d}(Fu_d, Fv_d)$, induced by the monopile can be expressed in the x and y directions as :

$$Fu_d(z) = -\frac{1}{2}\frac{\rho_0 C_d D}{\Delta x \Delta y}\|\mathbf{u}_\infty(\mathbf{z})\| u_\infty(z) \tag{6}$$

$$Fv_d(z) = -\frac{1}{2}\frac{\rho_0 C_d D}{\Delta x \Delta y}\|\mathbf{u}_\infty(\mathbf{z})\| v_\infty(z) \tag{7}$$

where C_d is the drag coefficient, D is the diameter of the pile, $\mathbf{u}_\infty(u_\infty, v_\infty)$ is the undisturbed current velocity upstream the pile, Δx and Δy are the size of the cell. These terms, divided by the density ρ_0, are added to the right hand side of momentum equations 1 and 2 respectively.

The turbulence equations become :

$$\frac{\partial k}{\partial t} + u\frac{\partial k}{\partial x} + v\frac{\partial k}{\partial y} = \frac{\partial}{\partial z}\left(\frac{\nu_V}{s_k}\frac{\partial k}{\partial z}\right) + P - \epsilon + \frac{\|\mathbf{u}_{\infty(\mathbf{z})}\|\|\mathbf{F_d}(\mathbf{z})\|}{\rho_0} \tag{8}$$

$$\frac{\partial \psi}{\partial t} + u\frac{\partial \psi}{\partial x} + v\frac{\partial \psi}{\partial y} = \frac{\partial}{\partial z}\left(\frac{\nu_V}{s_\psi}\frac{\partial \psi}{\partial z}\right) + \frac{\psi}{k}\left(C_1 P - C_2 \epsilon F_{wall} + C_2\frac{\|\mathbf{u}_{\infty(\mathbf{z})}\|\|\mathbf{F_d}(\mathbf{z})\|}{\rho_0}\right) \tag{9}$$

The distance between the pile and the location (i_∞, j_∞) where the velocity is considered equal to $\mathbf{u}_\infty$ was determined using the dry points approach for a pile with a diameter of 6 m and input velocities ranging between 0.3 and 1.2 m/s. Velocities were considered undisturbed when they are superior or equal to 99 % of the input velocity. Being based of these tests, the velocity is taken 90 m upstream the pile to estimate $\mathbf{u}_\infty$.

III – Applications

III – 1 Hydrodynamic test case

III – 1.1 Configurations

The domain is a square of 600 m with a water depth of 30 m. The horizontal resolution is 3 m and the water column is divided into 15 uniform layers. At the western boundary, sea surface heights vary periodically between 2 and -2 m to reproduce a tidal current typical from the Courseulles-sur-Mer site. Zero velocity gradient are applied along the eastern and western boundaries, and periodic boundary conditions are used along the northern and southern boundaries. A pile with a diameter equal to 6 m is placed in the middle of the domain. The order of magnitude of Reynolds number is 10^6. C_d is chosen equal to 0.65, compatible with the measurements made by [1] for this range of Reynolds numbers and the value taken by [15] in the Baltic Sea. f_{visc} is taken equal to 1.5. The size of the mesh being uniform, the horizontal viscosity is also uniform.

III – 1.2 Results

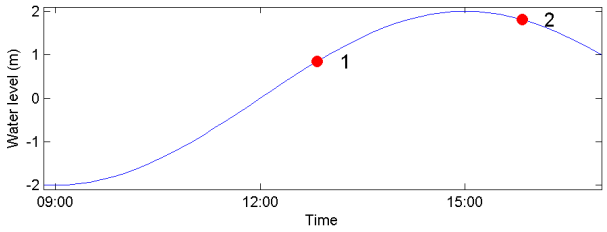

Figure 1 – Sea surface height (m) during simulation.

The barotropic velocity (Fig. 2), the near-bed velocity and turbulent kinetic energy (Fig. 3 and 4) are shown during the flow and just after the high tide (times 1 and 2, respectively, in Fig. 1). The background velocity is higher during the flow than at high tide, as expected. With the dry points strategy, the barotropic and near-bed velocities increase on both sides of the monopile due to the contraction of the flow, and decrease upstream the monopile. These monopile effects are consistent with those described by [17]. In front of the monopile, a horseshoe vortex is expected near the bed. [17] evaluated the size of this horseshoe vortex to be inferior to one time the diameter for a Reynolds number around 10^6. With our spatial resolution of 3 m, and a monopile with a diameter equal to 6 m, this corresponds to less than two cells and is thus difficult to reproduce. Downstream of the monopile, the barotropic velocity becomes null.

The pattern of barotropic velocity is properly reproduced with the parameterization (Fig 2). In the near-bed, the form of the wake behind the monopile differs between dry points method and parameterization. When the current is in the direction of the longitudinal axis (time 1, Fig 3, top), the differences are small and located mainly downstream in the immediate vicinity of the monopile. The pattern and intensity of the wake are still globally reproduced. However, in case of an oblique current, the velocity increases just behind the monopile, when it was expected to decrease (time 2, Fig 4, top).

The turbulent kinetic energy (TKE) close to the bottom increases around the monopile in both locations, especially upstream (Fig. 3 and 4, bottom). This agrees with [9], who measured an increase of turbulence close to the bottom upstream of a cylinder, up to a distance equal to one diameter. Results from the simulations are consistent with these

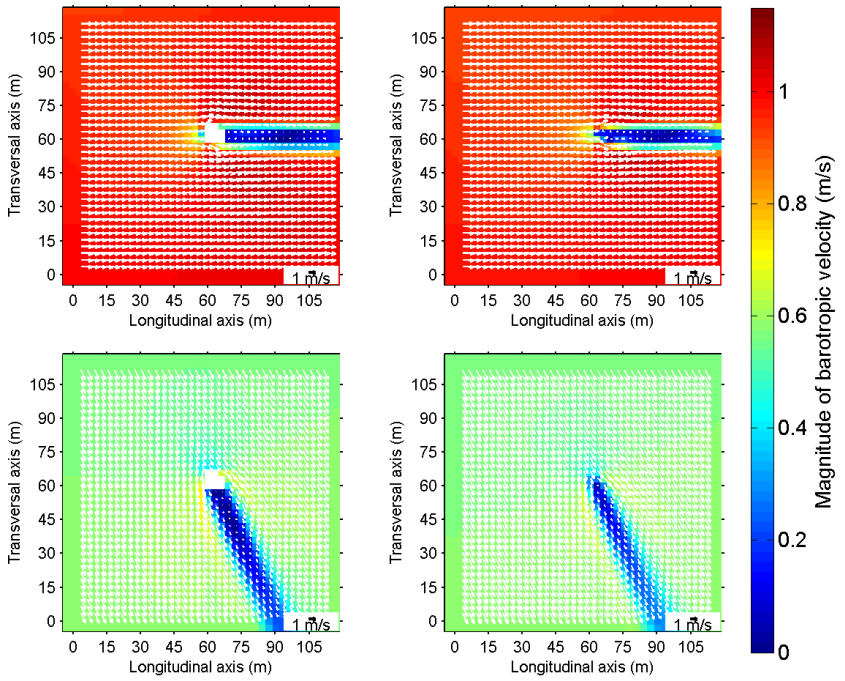

Figure 2 – Magnitude (m/s) and direction of barotropic velocity for t=1 (top) and t=2(bottom) with dry points approach (left) and parameterization approach (right)

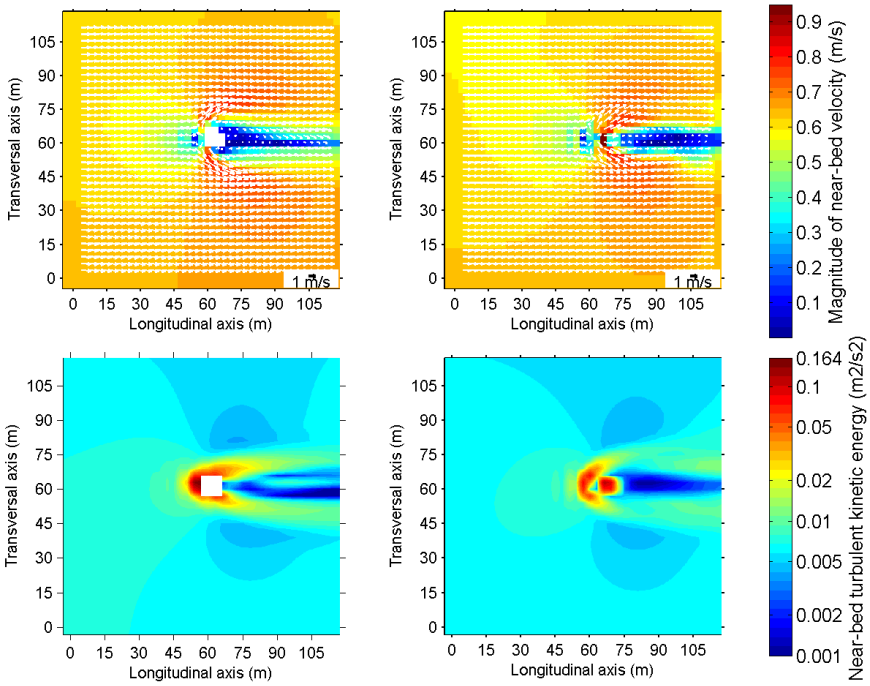

Figure 3 – Magnitude (m/s) and direction of near-bed velocity (top) and turbulent kinetic energy near-bead (bottom, $m^2.s^{-2}$, log scale) for t=1 with dry points approach (left) and parameterization approach (right)

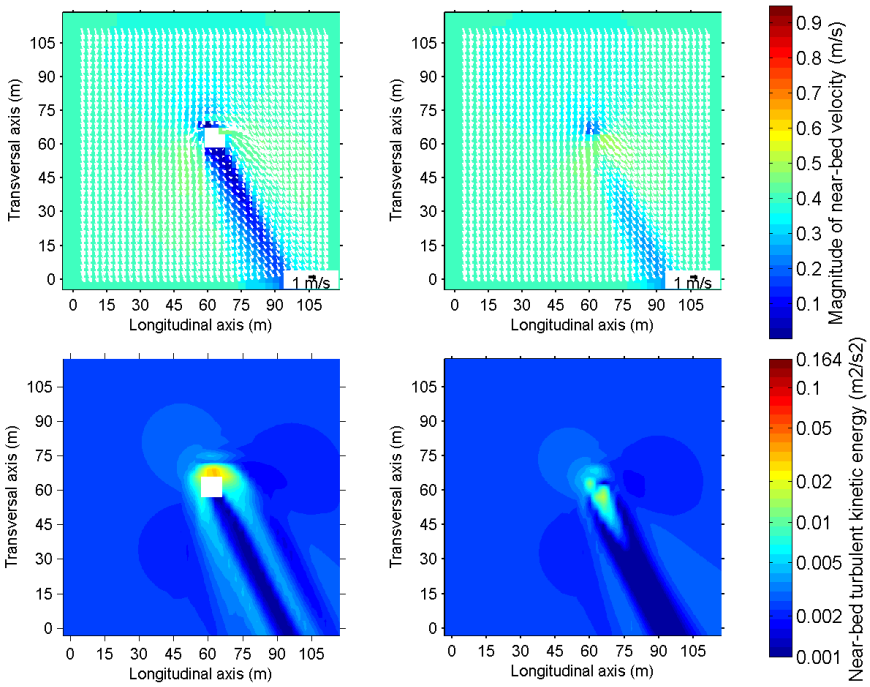

Figure 4 – Magnitude (m/s) and direction of near-bed velocity (top) and turbulent kinetic energy near-bead (bottom, $m^2.s^{-2}$, log scale) for t=2 with dry points approach (left) and parameterization approach (right)

measurements. At time 1 (Fig. 3), pattern of TKE, like velocity, are globally similar between the parameterization and the explicit method. However, at time 2, the near-bed TKE (Fig. 4, bottom) is stronger with the parameterization than with explicit method downstream close to the monopile, while it is weaker upstream of the monopile. This can explain the difference of velocity between the two methods visible at the top of figure 4.

III – 2 Sediment test case

III – 2.1 Configuration

The domain, the vertical and horizontal resolutions, the water depth and the monopile are the same as those for the hydrodynamic test case. A constant eastward current of 0.6 m/s is applied at the boundaries. The bed, with an initial thickness of 0.1 m, is composed of homogeneous sand with a diameter equal to 250 μm which is present in the Courseulles-sur-Mer site. Only suspended sediment transport are considered. The critical shear stress for erosion and the settling velocity are calculated following [19] and [18] respectively.

III – 2.2 Results

The pattern of the near-bed concentration (Fig. 5, top) is closely linked with the distribution of the bed shear stress (Fig. 5, middle). Near bed concentrations of suspended sediment calculated with both methods are higher at the side edge, where the bed shear stress is stronger, and null downstream of the monopile, where the bed shear stress is lower than the critical bed shear stress for erosion. In front of the monopile, the sediment concentration and the bed shear stress are also weak. This spatial distribution of bed shear stress is in agreement with [17] and [9]. The bed is eroded at the side edge of monopile and sand deposits downstream at the side edge of the wake, where the bed shear stress

becomes weaker(Fig. 5, bottom). In front of the pile, the bed is not eroded as expected [17].This can be explained by the fact that horseshoe vortices are not reproduced in the model because of resolution.

Patterns are different between the dry point method and the parameterization method, especially in the immediate vicinity of the monopile. This difference is expected, due to the discrepancies in the near-bed velocities between the two methods at this location, discussed in section III-1.

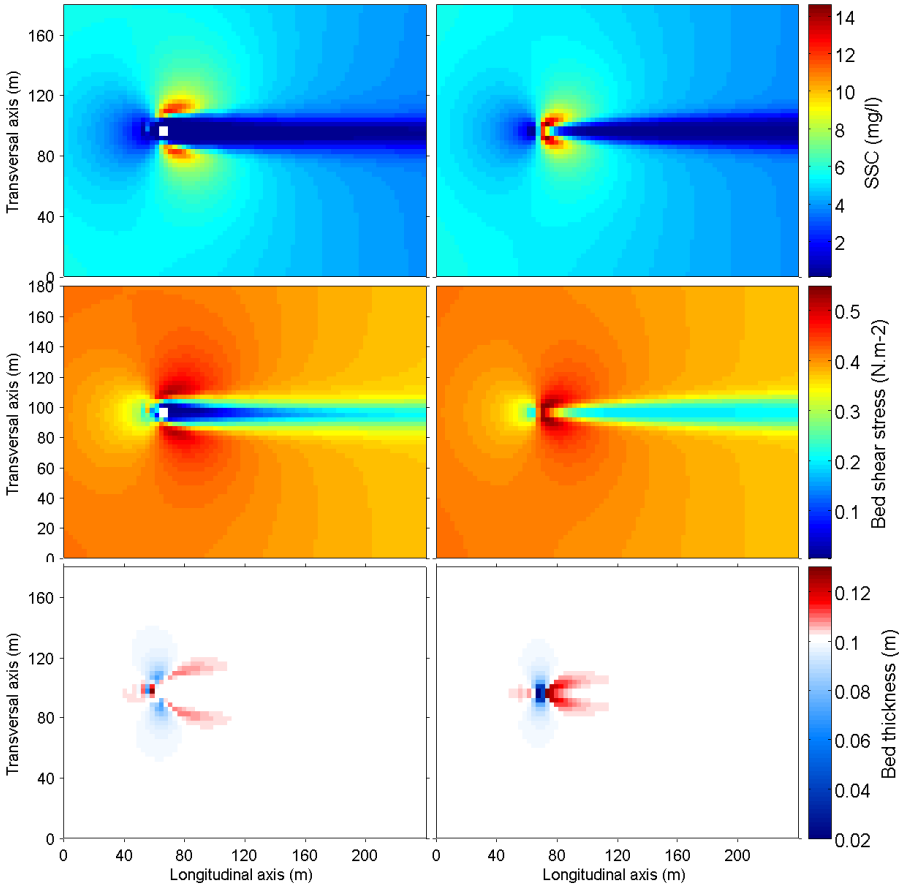

Figure 5 – Suspended sand concentration in the near-bed (SSC, mg/l, top), bed shear stress (N.m^{-2}, middle) and bed thickness (m, bottom) after 11 hours of simulation with dry points approach (left) and parameterization approach (right).

III – 3 Courseulles-sur-Mer

III – 3.1 Configuration

The regional model MARS3D is applied in a domain including the future offshore wind farm of Courseulles-sur-Mer (Fig. 6). Five nested ranks are used to allow a high resolution and take into account explicitly the monopile in the mesh. The horizontal resolutions are 243 m for rank 0 (red grid), 81 m for rank 1 (green grid), 27 m for rank 2 (pink grid), 9 m for rank 3 (blue grid) and 3 m for rank 4 (brown grid). The sea surface height is forced by data from SHOM (French Navy) for rank 0 and by data from the previous rank for the other ranks. Zero velocity gradients are imposed along open boundaries for rank 0. Dirichlet conditions are used for velocities for the other ranks. Only the rank 4 is

solved in three-dimensions. Simulations are carried out on the 13/11/2011 when the tide is medium (tidal coefficient of 78). In the regional simulation case (with nested ranks), the horizontal viscosity had to be increased to avoid numerical instabilities. f_{visc} is taken equal to 10, leading to a uniform horizontal viscosity equal to 0.35 m^2/s with a uniform spatial resolution.

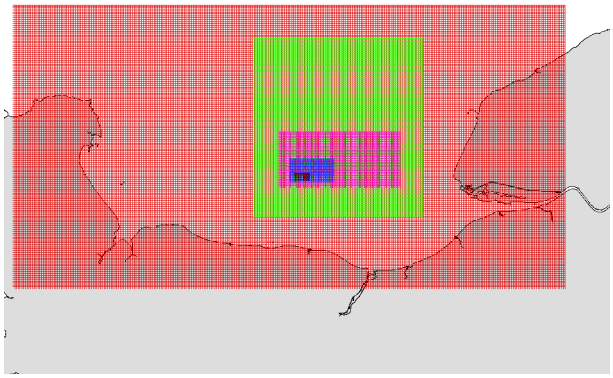

Figure 6 – Calculation domains for the regional scale

III – 3.2 Results

Figure 7 shows the magnitude of the barotropic velocity with the dry points approach at 15 :00 when the velocity reachs its maximum value during the semi-diurnal tidal cycle. A wake appears downstream of each of the monopiles. A zoom is shown in figure 8 to analyse the pattern. With the dry points method (Fig. 8, top),the barotropic velocity decreases both in front and downstream of the monopile, but increases on the sides, in agreement with the results found in section 3.1. However, the decrease in velocity is smaller in this case than in the test case (Fig. 2). This is due to the higher input horizontal viscosity used in this case. With the parameterization when the drag coefficient is still equal to 0.65 (Fig. 8, middle), the spatial distribution of the barotropic velocity is reproduced but the impact is underestimated. The drag coefficient has to be increased to 1 (Fig. 8, bottom) to reach the same order of magnitude for the velocity in dry points method and parameterization method, while keeping the same pattern. The increase of the horizontal viscosity reduces and softens the effect of drag force on the flow. An artificial increase of C_d is needed to produce the correct drag force.

IV – Discussion

The dry points strategy is considered here as the reference method. However, velocities obtained with this method still have to be validated. The width of the wake predicted with this method is compared with experimental measurements described in [4], following a Froude similarity criterion. Figure 9 indicates that the intensity of the streamwise component of velocity across the flume near the surface is correctly reproduced. Moreover physical modelling at laboratory scales is being performed by project partners at the universities of Caen, Le Havre and Plymouth, in order to validate further the numerical modelling.

The drag coefficient C_d is taken constant in the test cases. However, the parameterization either underestimates or overestimates the wake behind the monopile depending

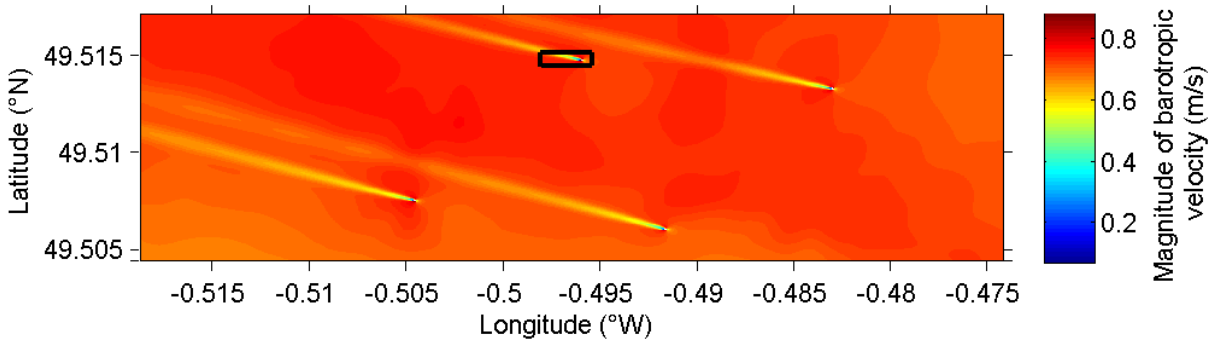

Figure 7 – Magnitude of barotropic velocity (m/s) for Courseulles-sur-Mer site with dry points approach the 13/11/2011 at 15 :00. The rectangular frame indicates the area where the zoom is shown in figure 8.

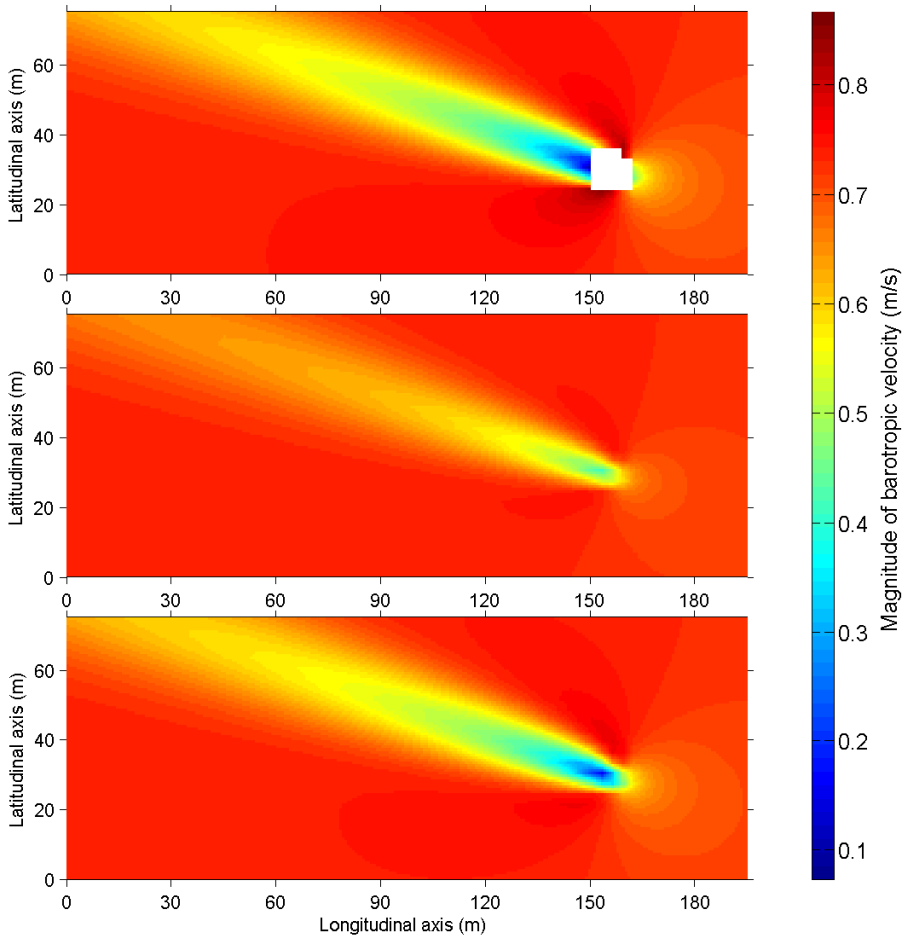

Figure 8 – Zoom of the Magnitude (m/s) of barotropic velocity (m/s) the 13/11/2011 at 15 :00 for Courseulles-sur-Mer with dry points approach (top) and parameterization approach with $C_d = 0.65$ (middle) and $C_d = 1$ (bottom).

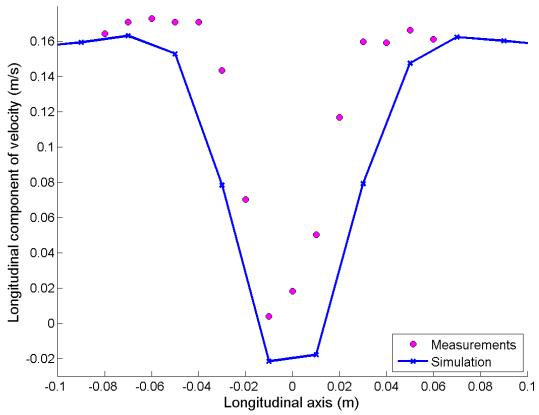

Figure 9 – Streamwise component of velocity (m/s) across the flume near the surface simulated (blue line) and measured (pink points).

of velocity. This can be explained by the fact that C_d is very sensitive for this range of Reynolds numbers [1, 2, 16]. The values of the drag coefficient C_d, used in the parameterization method, should vary as a function of the Reynolds number, to improve results along an entire tidal cycle. The monopile shape and and the flow direction also influence the drag coefficient (e.g. [14]).

The parameterization method has difficulties in reproducing the pattern of the near-bed velocities around the monopile. At this location, complex structures, such as horseshoe vortices, are observed upstream of the monopile. These vortices are well reproduced by [17], who solve explicitly the monopile and use a very high model resolution, with 128 cells all around monopile perimeter. At present, the parameterization method developed here doesn't take into account this source of turbulence. However, as indicated in section 3.1, the size of the horseshoe vortex is less than one diameter [17], so less than the size of two cells with the resolution used in our study. A sub-grid parameterization using a coarse grid is not able to reproduce horseshoe vortices.

The undisturbed (free stream) velocity is taken 90 m away from the monopile. However, in the regional model case, modifications of the current between this point and the monopile, due for instance to bathymetric changes, are not take into account. This distance may be reduced in regional cases to calculate the drag force with an appropriate velocity.

Improvements of the parameterization method will help to reproduce the impact of a monopile on the hydrodynamics more accurately, especially at the bottom, and will lead to a better estimation of the sediment transport. Indeed, erosion and deposition are closely linked to the current velocity, and are key factors to evaluate the suspended sediment concentrations for this type of sand. For the regional case, the heterogeneity of the sediment, and the contributions of sediment discharges coming from rivers (Seine, Orne, Baie des Veys) or from coastal erosion [23], will have to be considered.

V – Conclusions

In this paper two methods to assess monopile impacts on hydrodynamics and sediment transport were presented : a first approach explicitly solving the monopile, and a second approach where the effect of the monopile is included as a parameterization. The spatial distributions of velocity and TKE simulated with the first approach are in agreement

with those published. The parameterization approach generally reproduces the velocity and TKE, but improvements are needed in the near-bed. It was observed that the choice of the drag coefficient for high Reynolds numbers requires further developments. Also, knowledge of the near-bed velocity around the monopile is essential to estimate local scour. Future work will consider the effect of waves on the monopile impacts, by coupling the circulation model MARS3D with the sea state model WW3 [6].

VI – Acknowledgments

This paper is a contribution to the European cross-border program Interreg IVA France (Channel) - England OFELIA (Offshore Foundations EnvironmentaL Impact Assessments), which involves the universities of Caen, Le Havre and Plymouth. A. Rivier and G. Pinon are supported by the University of Le Havre, A.C. Bennis by the University of Caen and V. Magar and M. Gross by CICESE. A. Rivier acknowledges the support of a post-doctoral grant from the University of Le Havre. The authors are grateful to Frank Dumas (IFREMER) for providing the model configuration for the Courseulles-sur-Mer site and to Alexander Ezersky (University of Caen) for providing experimental data.

Références

[1] E. Achenbach. Distribution of local pressure and skin friction around a circular cylinder in cross-flow up to Re= 5×10^6. *Journal of Fluid Mechanics*, 34(04) :625–639, 1968.

[2] E. Achenbach. Influence of surface roughness on the cross-flow around a circular cylinder. *Journal of Fluid Mechanics*, 46(02) :321–335, 1971.

[3] Actimar. Synthèse de l'étude 2009 - Analyse des impacts hydrosédimentaires du projet de parc éolien en mer en Baie de Seine,rapport moc n°0732 prepared for Eoliennes offshore du Calvados, 2013.

[4] A. Baelhaq. Traitement des données expérimentales sur la synchronisation d'allée de Von Karman par les ondes superficielles. Master's thesis, Université de Caen Basse-Normandie, 2014.

[5] M. Baptist, V. Babovic, J. Rodríguez Uthurburu, M. Keijzer, R. Uittenbogaard, A. Mynett, and A. Verwey. On inducing equations for vegetation resistance. *Journal of Hydraulic Research*, 45(4) :435–450, 2007.

[6] A.-C. Bennis, F. Ardhuin, and F. Dumas. On the coupling of wave and three-dimensional circulation models : Choice of theoretical framework, practical implementation and adiabatic tests. *Ocean Modelling*, 40(3) :260–272, 2011.

[7] T. Bouma, L. Van Duren, S. Temmerman, T. Claverie, A. Blanco-Garcia, T. Ysebaert, and P. Herman. Spatial flow and sedimentation patterns within patches of epibenthic structures : Combining field, flume and modelling experiments. *Continental Shelf Research*, 27(8) :1020–1045, 2007.

[8] CEFAS. Scroby Sands Offshore Wind Farm - Coastal Processes Monitoring. Final Report AEO262 prepared for Marine Environmental Division, Defra and Department of Trade and Industry, 2006.

[9] B. Dargahi. The turbulent flow field around a circular cylinder. *Experiments in Fluids*, 8(1-2) :1–12, 1989.

[10] Department of Energy and Climate Change. Review of Round 1 sediment process monitoring data - lessons learnt, Final Report, 2008.

[11] DHI. Horns Rev Wind Power Plant. Environmental impact assessment of hydrography. Report prepared for ELSAMPROJEKT, 1999.

[12] P. Lazure and F. Dumas. external–internal mode coupling for a 3D hydrodynamical model for applications at regional scale (MARS). *Advances in Water Resources*, 31(2) :233–250, 2008.

[13] P. Le Hir, F. Cayocca, and B. Waeles. Dynamics of sand and mud mixtures : a multiprocess-based modelling strategy. *Continental Shelf Research*, 31(10) :S135–S149, 2011.

[14] W. Lindsey. *Drag of cylinders of simple shapes*. NACA, 1938.

[15] H. Rennau, S. Schimmels, and H. Burchard. On the effect of structure-induced resistance and mixing on inflows into the Baltic Sea : A numerical model study. *Coastal Engineering*, 60 :53–68, 2012.

[16] A. Roshko. Experiments on the flow past a circular cylinder at very high Reynolds number. *Journal of Fluid Mechanics*, 10(03) :345–356, 1961.

[17] A. Roulund, B. M. Sumer, J. Fredsøe, and J. Michelsen. Numerical and experimental investigation of flow and scour around a circular pile. *Journal of Fluid Mechanics*, 534 :351–401, 2005.

[18] R. Soulsby. *Dynamics of marine sands : a manual for practical applications*. Thomas Telford, 1997.

[19] R. Soulsby and R. Whitehouse. Threshold of sediment motion in coastal environments. In *Pacific Coasts and Ports' 97 : Proceedings of the 13th Australasian Coastal and Ocean Engineering Conference and the 6th Australasian Port and Harbour Conference ; Volume 1*, page 145. Centre for Advanced Engineering, University of Canterbury, 1997.

[20] S. Temmerman, T. Bouma, G. Govers, Z. Wang, M. De Vries, and P. Herman. Impact of vegetation on flow routing and sedimentation patterns : Three-dimensional modeling for a tidal marsh. *Journal of Geophysical Research : Earth Surface (2003–2012)*, 110(F4), 2005.

[21] L. Umlauf and H. Burchard. A generic length-scale equation for geophysical turbulence models. *Journal of Marine Research*, 61(2) :235–265, 2003.

[22] Q. Vanhellemont and K. Ruddick. Turbid wakes associated with offshore wind turbines observed with Landsat 8. *Remote Sensing of Environment*, 145 :105–115, 2014.

[23] A. Velegrakis, D. Michel, M. Collins, R. Lafite, E. Oikonomou, J. Dupont, M. Huault, M. Lecouturier, J. Salomon, and C. Bishop. Sources, sinks and resuspension of suspended particulate matter in the eastern English Channel. *Continental Shelf Research*, 19(15) :1933–1957, 1999.